

Alkali metal clusters by DFT

Jacopo Cocomello, Antonio Anna Mele, Luca Zuanazzi

May 2020

Introduction

Consider alkali metal clusters that are produced in jets of vaporized metal. We use the density functional theory to study shell effects on the clusters, experimentally observed in the mass spectrum of the jets. We model each cluster of N atoms as a sphere of uniform positive charge (jellium) with density ρ_B and containing N electrons. The size of a cluster is given by $\frac{4}{3}\pi R_c^3 \rho_B = N$ while the density is in turn parametrized by the Wigner-Seitz radius $\frac{4}{3}\pi R_s^3 \rho_B = 1$. Throughout the whole exercise we will use atomic units, this means to set $\hbar = 1$, $e = 1$, $m_e = 1$ and $4\pi\epsilon_0 = 1$. Lengths will then be expressed in Bohr radii $a_0 = 4\pi\epsilon_0\hbar^2/me^2$ and energies in Hartrees $E_h = \hbar^2/ma_0^2$.

We recall that, in a DFT calculation, the energy functional has the form

$$E[\rho] = T[\rho] + V_{ext}[\rho] + V_{int}[\rho] + E_{xc}[\rho] \quad (1)$$

while the wave function of the system consists in a Slater determinant of single particle states, hence the one body density reads

$$\rho(r) = \sum_{i=1}^N |\phi_i(\mathbf{r})|^2 \quad (2)$$

The first term in equation (1) is the kinetic energy

$$T[\rho] = -\frac{1}{2} \sum_i \int \phi_i^*(\mathbf{r}) \nabla^2 \phi_i(\mathbf{r}) d^3r \quad (3)$$

then we have the external and internal potentials, which in our case turn out to be respectively

$$V_{ext}[\rho] = \int \rho(r) V_{ext}(r) d^3r, \quad V_{ext}(r) = 2\pi\rho_B \left[\left(\frac{r^2}{3} - R_c^2 \right) \Theta(R_c - r) - \frac{2R_c^3}{3r} \Theta(r - R_c) \right] \quad (4)$$

$$V_{int}[\rho] = \frac{1}{2} \int \rho(r) V_{int}(r) d^3r, \quad V_{int}(r) = 4\pi \left[\int_0^r \rho(r') \frac{r'^2}{r} dr' + \int_r^\infty \rho(r') r' dr' \right] \quad (5)$$

Lastly, there is the exchange-correlation energy

$$E_{xc}[\rho] = \int [\epsilon_x(r) + \epsilon_c(r)] \rho(r) d^3r \quad (6)$$

with

$$\epsilon_x(r) = -\frac{3}{4} \left(\frac{3}{\pi} \rho(r) \right)^{\frac{1}{3}} \quad \epsilon_c(r) = \frac{\gamma}{1 + \beta_1 \sqrt{r_s} + \beta_2 r_s} \quad (7)$$

r_s being the Wigner-Seitz radius relative to the electron density ρ . This form of correlation energy is called Perdew-Zunger¹ parametrization and the parameters, valid for an unpolarized system, are taken from the Quantum Monte Carlo calculations of Ortiz and Ballone² and read $\gamma = -0.103756 E_h$, $\beta_1 = 0.56371 a_0^{-1/2}$, $\beta_2 = 0.27358 a_0^{-1}$.

The minimization of the energy (1) leads to the Kohn-Sham equation

$$\left[-\frac{1}{2} \nabla^2 + V_{ext}(r) + V_{int}(r) + \frac{\delta E_{xc}[\rho]}{\delta \rho} \right] \phi_i(\mathbf{r}) = \mu_i \phi_i(\mathbf{r}) \quad (8)$$

Given the spherical symmetry of the problem we write the single particle states as

$$\phi_i(\mathbf{r}) = \frac{u_{n,l}(r)}{r} Y_{l,m}(\Omega) |s=\frac{1}{2}, m_s\rangle \quad (9)$$

¹J.P. Perdew and A. Zunger, Phys. Rev. B 23, 5048 (1981)

²G. Ortiz and P. Ballone, Phys. Rev. B 30, 1391 (1994)

so that the Kohn-Sham equation becomes

$$\left[-\frac{1}{2} \frac{d^2}{dr^2} + \frac{l(l+1)}{2r^2} + V_{ext}(r) + V_{int}(r) + \frac{\delta E_{xc}[\rho]}{\delta \rho} \right] u_{n,l}(r) = \mu_{n,l} u_{n,l}(r) \quad (10)$$

Non-interacting electron model

Here we neglect the electron-electron interaction and consider only the external potential. We then remain with a simple radial Schrödinger equation

$$\left[-\frac{1}{2} \frac{d^2}{dr^2} + \frac{l(l+1)}{2r^2} + V_{ext}(r) \right] u_l(r) = \mu_l u_l(r) \quad (11)$$

which can be solved with the Numerov's method. We will study clusters of sodium, for which $R_s(\text{Na}) = 3.93 a_0$, or potassium, $R_s(\text{K}) = 4.86 a_0$.

The first four energy levels we obtain solving the Schrödinger equation are $1s$, $1p$, $2s$ and $1d$ both for Na and K. Notice that in principle the ordering of the energy levels may vary with N , since V_{ext} depends on it. Luckily for us, in this case the energy levels do not mix for $N \leq 20$. This means that the first four closed shells correspond to a system in which the states $1s$, $1p$, $2s$ and $1d$ are completely occupied. That is a system with $N = 2, 8, 10$ or 20 electrons, considering the degeneracy of orbital angular momentum and spin.

For example, the density of the second closed shell reads

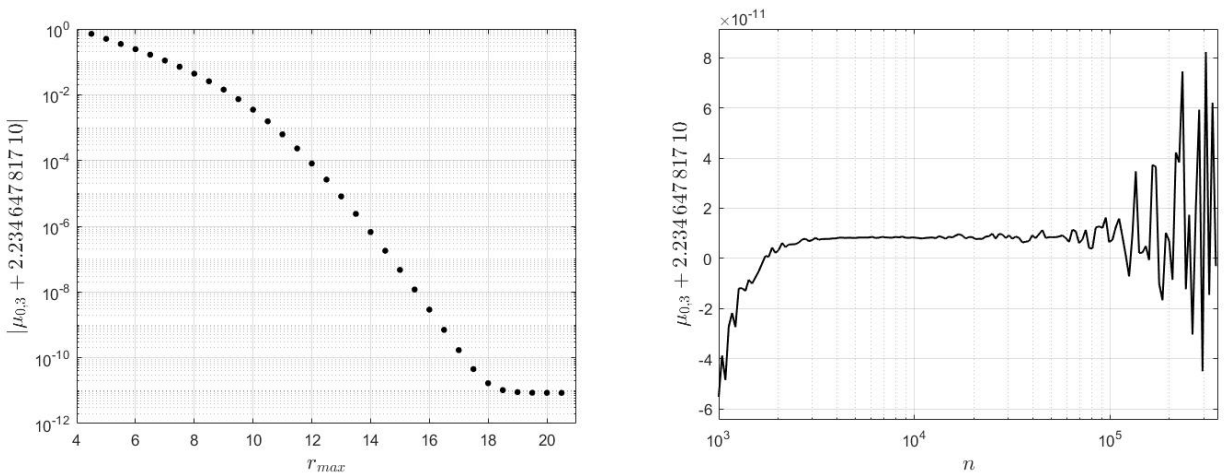
$$\rho(r) = 2 \left[\frac{u_{0,0}^2}{r^2} |Y_{0,0}|^2 + \frac{u_{0,1}^2}{r^2} (|Y_{1,-1}|^2 + |Y_{1,0}|^2 + |Y_{1,1}|^2) \right] = \frac{2}{4\pi r^2} (u_{0,0}^2 + 3u_{0,1}^2) \quad (12)$$

where we have used the formula

$$\sum_{m=-l}^l |Y_{l,m}|^2 = \frac{2l+1}{4\pi} \quad (13)$$

Notice that in this way all densities relative to a closed shell depend only on the modulus r , respecting the spherical symmetry of the system.

In Figure 1 we show the convergence of a particular representative eigenvalue, $\mu_{0,3}$ for a cluster of $N = 20$ sodium atoms, varying the mesh parameters n and r_{max} .



(a) We vary r_{max} keeping $h = 3 \times 10^{-3}$.

(b) We vary n keeping $r_{max} = 30$.

Figure 1: Convergence of $\mu_{0,3}$ for a cluster of $N = 20$ sodium atoms. The mesh is such that $nh = r_{max}$.

From Figure 1a we can see that, even though the potential has a long tail and slowly converges to zero, the eigenvalues don't need a too long mesh to converge. Instead from 1b we deduce that a too big n , that is a too small h , leads to considerable numerical errors.

In Figure 2 we plot the densities of the first four closed shells of sodium and potassium.

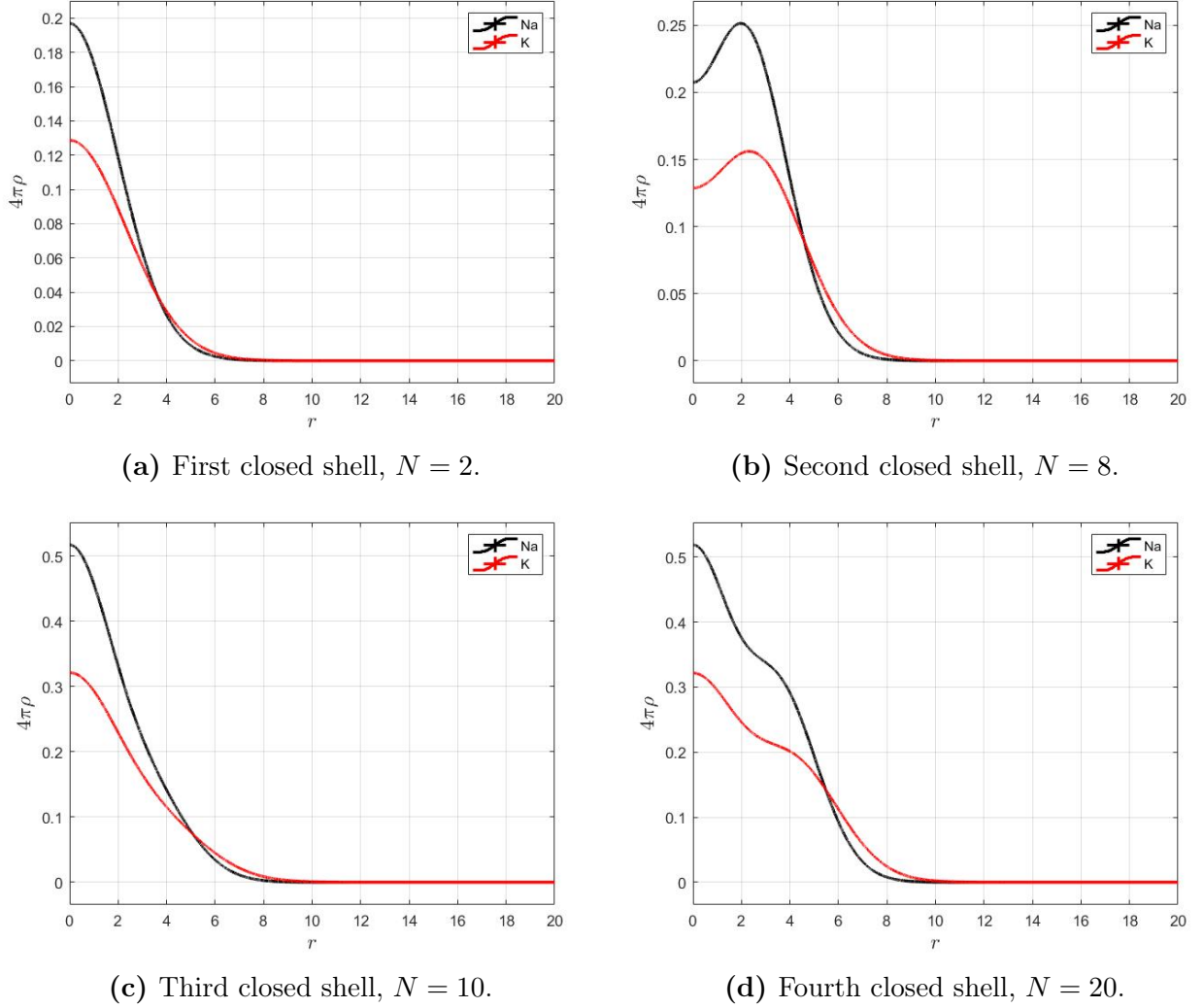


Figure 2: First four closed shells for sodium and potassium.

Laslty, we compute the total energy of the different clusters, in this non-interacting model we simply have $E = \sum_i \mu_i$.

	$N = 2$	$N = 8$	$N = 10$	$N = 20$
$\mu_{0,0}$	-0.416 108 010 15	-1.334 199 142 70	-1.579 070 479 17	-2.619 706 014 31
$\mu_{0,1}$	-0.297 848 150 68	-1.205 930 574 82	-1.450 741 073 69	-2.491 351 625 72
$\mu_{1,0}$	-0.215 275 798 05	-1.078 347 257 65	-1.322 640 636 62	-2.362 999 144 50
$\mu_{0,2}$	-0.196 530 631 26	-1.077 935 883 17	-1.322 503 161 08	-2.362 997 999 95
E	-0.832 216 020 30	-9.903 981 734 32	-14.507 868 673 72	-48.543 500 071 44

Table 1: Single particle and total energy for different sodium clusters.

	$N = 2$	$N = 8$	$N = 10$	$N = 20$
$\mu_{0,0}$	-0.351 251 437 32	-1.094 568 842 89	-1.292 587 156 36	-2.134 090 676 26
$\mu_{0,1}$	-0.262 974 003 49	-1.001 260 074 25	-1.199 258 668 68	-2.040 755 467 29
$\mu_{1,0}$	-0.194 837 462 36	-0.908 183 284 74	-1.105 998 064 33	-1.947 420 572 29
$\mu_{0,2}$	-0.183 770 630 80	-0.908 043 998 81	-1.105 957 312 01	-1.947 420 383 91
E	-0.702 502 874 64	-8.196 698 131 28	-11.992 722 453 46	-39.881 759 139 94

Table 2: Single particle and total energy for different potassium clusters.

Exchange and correlation potentials

We want to find a form for the exchange and correlation potentials which enter in (10) as

$$\frac{\delta E_{xc}[\rho]}{\delta \rho} = \rho(r) \frac{\partial}{\partial \rho} (\epsilon_x + \epsilon_c) + \epsilon_x(r) + \epsilon_c(r) \quad (14)$$

The exchange Coulomb term can be obtained from the Fourier transform of Coulomb potential integrated over the Fermi sphere. The result is

$$\epsilon_x(r) = -\frac{3}{4} \left(\frac{3}{\pi} \rho(r) \right)^{\frac{1}{3}} \quad (15)$$

and the exchange energy functional is

$$E_x[\rho] = \int \epsilon_x(r) \rho(r) d^3r = -\frac{3}{4} \left(\frac{3}{\pi} \right)^{\frac{1}{3}} \int \rho(r)^{4/3} d^3r; \quad (16)$$

the exchange potential is obtained via functional derivative on $E_x[\rho]$ as

$$\frac{\delta E_x[\rho]}{\delta \rho} = -\left(\frac{3}{\pi} \right)^{\frac{1}{3}} \rho(r)^{1/3} = \frac{4}{3} \epsilon_x(r). \quad (17)$$

The correlation energy functional is obtained from

$$E_c[\rho] = \int \epsilon_c(r) \rho(r) d^3r, \quad (18)$$

with

$$\epsilon_c(r) = \frac{\gamma}{1 + \beta_1 \sqrt{r_s} + \beta_2 r_s}. \quad (19)$$

Notice that ϵ_c depends on r through the density as the Wigner-Seitz radius is defined by

$$r_s = \left(\frac{3}{4\pi\rho(r)} \right)^{\frac{1}{3}}, \quad (20)$$

hence the correlation potential is given by

$$\frac{\delta E_c[\rho]}{\delta \rho} = \epsilon_c(r) + \rho(r) \frac{\partial \epsilon_c}{\partial r_s} \frac{\partial r_s}{\partial \rho}. \quad (21)$$

The derivatives are easily evaluated

$$\frac{\partial \epsilon_c}{\partial r_s} = -\gamma \frac{\beta_2 + \frac{1}{2}\beta_1 r_s^{-1/2}}{(1 + \beta_1 \sqrt{r_s} + \beta_2 r_s)^2}, \quad \frac{\partial r_s}{\partial \rho} = -\frac{1}{3} \frac{r_s}{\rho} \quad (22)$$

hence the correlation potential becomes

$$\frac{\delta E_c[\rho]}{\delta \rho} = \epsilon_c + \frac{\gamma}{6} \frac{\beta_1 \sqrt{r_s} + 2\beta_2 r_s}{(1 + \beta_1 \sqrt{r_s} + \beta_2 r_s)^2} = \frac{\epsilon_c}{6} \left(\frac{6 + 7\beta_1 \sqrt{r_s} + 8\beta_2 r_s}{1 + \beta_1 \sqrt{r_s} + \beta_2 r_s} \right). \quad (23)$$

The Kohn-Sham equation explicitly becomes

$$\left[-\frac{1}{2} \frac{d^2}{dr^2} + \frac{l(l+1)}{2r^2} + V_{ext} + V_{int} + \frac{4}{3}\epsilon_x + \frac{\epsilon_c}{6} \left(\frac{6 + 7\beta_1 \sqrt{r_s} + 8\beta_2 r_s}{1 + \beta_1 \sqrt{r_s} + \beta_2 r_s} \right) \right] u_{n,l} = \mu_{n,l} u_{n,l} \quad (24)$$

Solution to the Kohn-Sham equation

To solve the Kohn-Sham equation we implement the self-consistent procedure represented by the flowchart in Figure 3. From the considerations on the convergence of the single orbital eigenvalues in the non-interacting model we choose a mesh with $n = 10000$ and $h = 3 \times 10^{-3}$, hence $r_{max} = 30$.

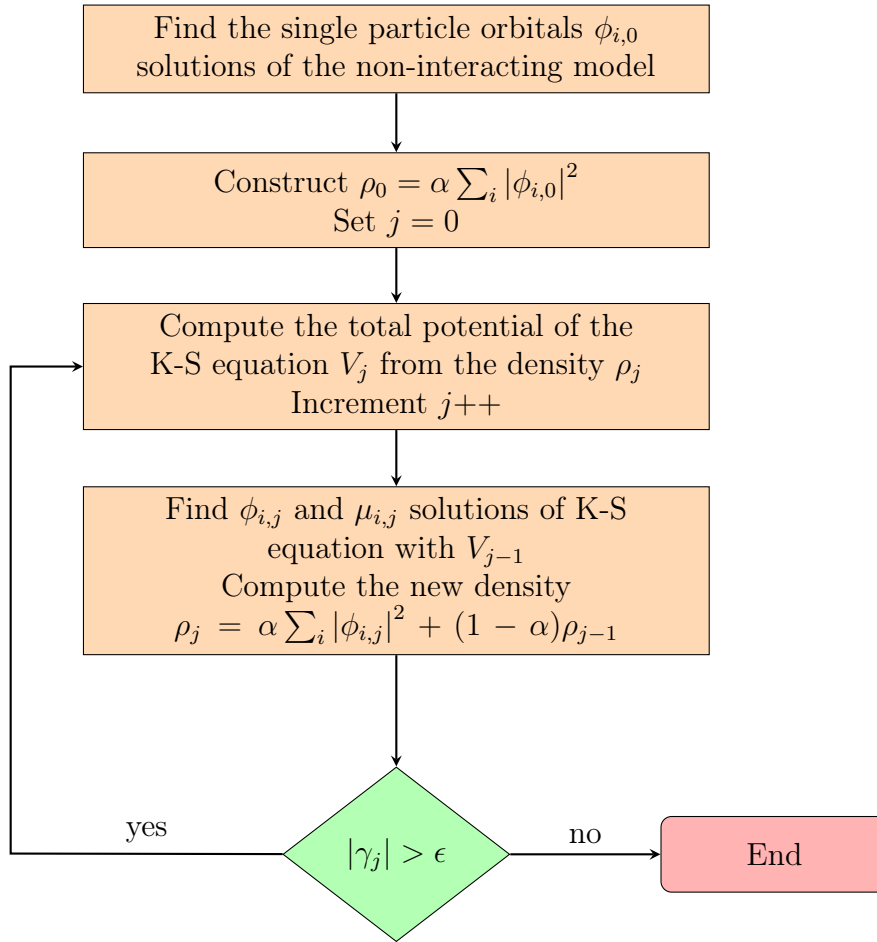


Figure 3: Flowchart of the self-consistent procedure.

Note that, from the definition of ρ_0 , the norm of the density starts from αN and converges to N through the procedure. Indeed we have

$$\int \rho_j(r) d^3 r = N \left[1 - (1 - \alpha)^{j+1} \right] \quad j = 0, 1, 2, \dots \quad (25)$$

We now explicit the convergence criterion written in the flowchart. It is well known that, if ρ is a solution to the Kohn-Sham equation, it holds the following

$$T[\rho] + V_{ext}[\rho] + 2V_{int}[\rho] + \int \rho(r) \frac{\delta E_{xc}[\rho]}{\delta \rho} d^3 r = \sum_i \mu_i \quad (26)$$

Exploiting the Kohn-Sham equation to get rid of the double derivative, the kinetic energy at the step j becomes

$$T[\rho_j] = \sum_i \int u_{n,l,j}^*(r) \left(-\frac{1}{2} \frac{d^2}{dr^2} + \frac{l(l+1)}{2r^2} \right) u_{n,l,j}(r) dr \quad (27)$$

$$= \sum_i \mu_{i,j} - \int \rho_j(r) \left(V_{ext}(r) + V_{int,j-1}(r) + \frac{\delta E_{xc}[\rho_{j-1}]}{\delta \rho} \right) d^3r \quad (28)$$

where $V_{int,j}$ is the interaction potential computed with ρ_j . Inserting this expression into (26) the convergence condition becomes

$$\gamma_j = \int \rho_j(r) \left(V_{int,j}(r) - V_{int,j-1}(r) + \frac{\delta E_{xc}[\rho_j]}{\delta \rho} - \frac{\delta E_{xc}[\rho_{j-1}]}{\delta \rho} \right) d^3r = 0 \quad (29)$$

During the self-consistent procedure, when the convergence condition is not satisfied, the total energy must be calculated from

$$E[\rho_j] = \sum_i \mu_{i,j} + \int \rho_j(r) \left(\frac{1}{2} V_{int,j}(r) - V_{int,j-1}(r) - \frac{\delta E_{xc}[\rho_{j-1}]}{\delta \rho} + \epsilon_{x,j}(r) + \epsilon_{c,j}(r) \right) d^3r \quad (30)$$

Numerical results

We solve the Kohn-Sham equation for clusters of $N = 8, 20$ and 40 sodium atoms. We will assume the first energy levels to be $1s, 1p, 2s, 1d, 2p$ and $1f$ throughout the whole self-consistent procedure. We set the parameter $\alpha = 0.1$.

In Figure 4 we plot the convergence criterion and the total energy as function of the iteration step j .

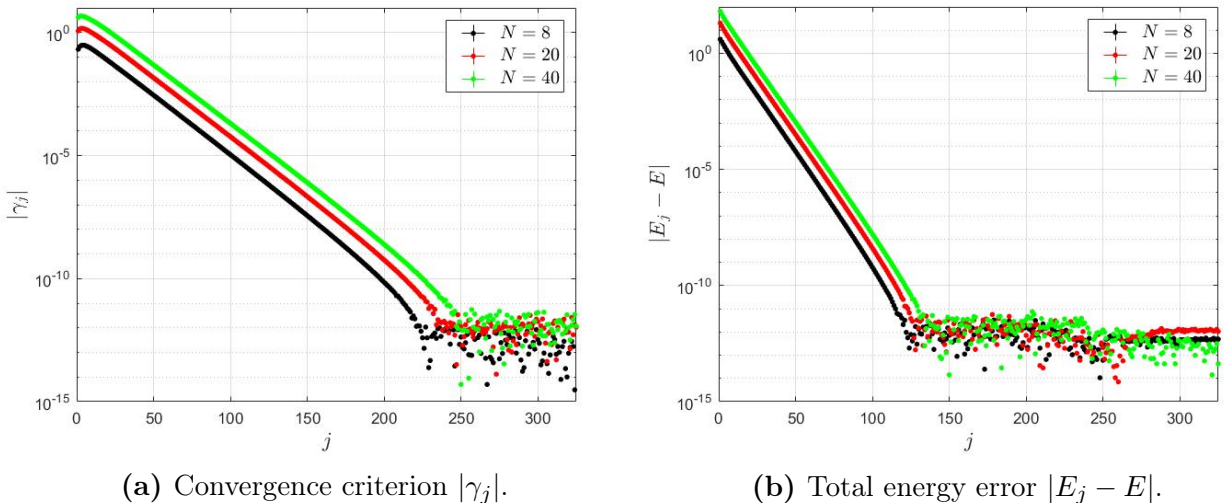
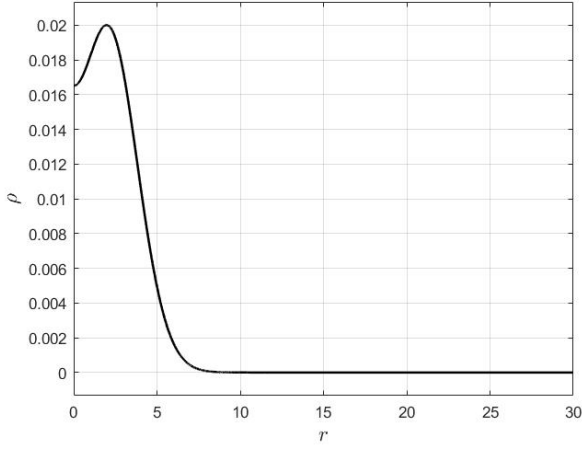


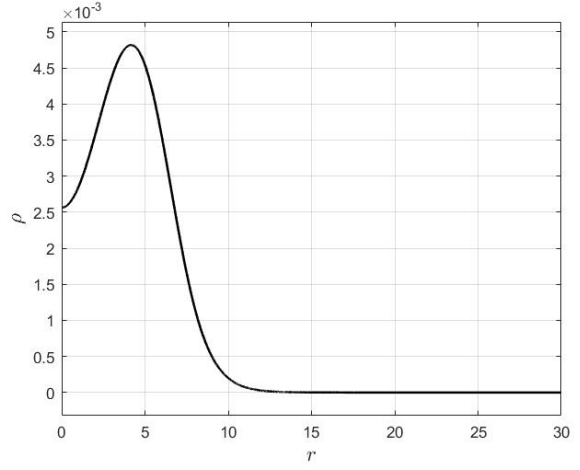
Figure 4: Convergence of the self-consistent procedure for different sodium clusters.

In Figure 4b we indicate with E the converging value of the energy, obtained averaging the numerical noise. Notice that the energy starts showing numerical fluctuations way before γ does.

In Figure 5 we compare the non-interacting solution with the Kohn-Sham solution. Both energy and density are presented.

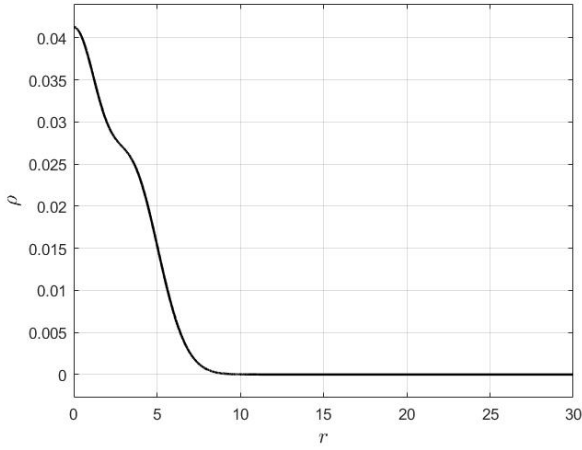


$$E = -9.903\,981\,734\,32$$

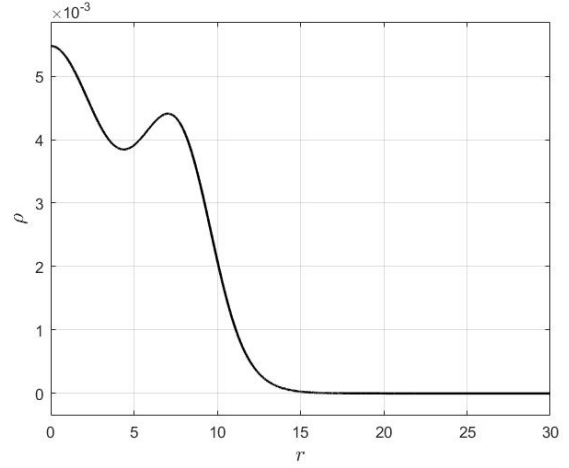


$$E = -5.422\,569\,717\,88$$

(a) Non-interacting solution on the left and Kohn-Sham solution on the right for $N = 8$.

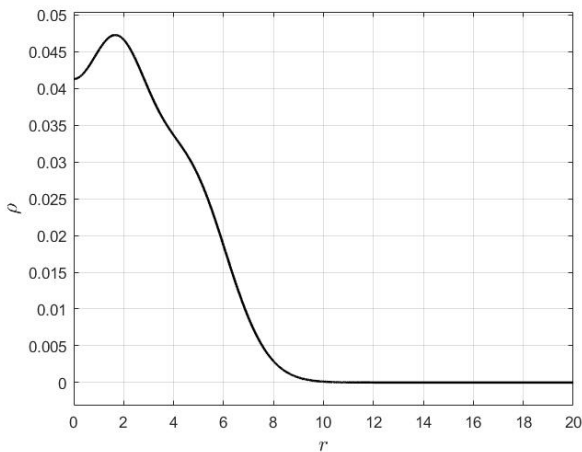


$$E = -48.543\,500\,071\,44$$

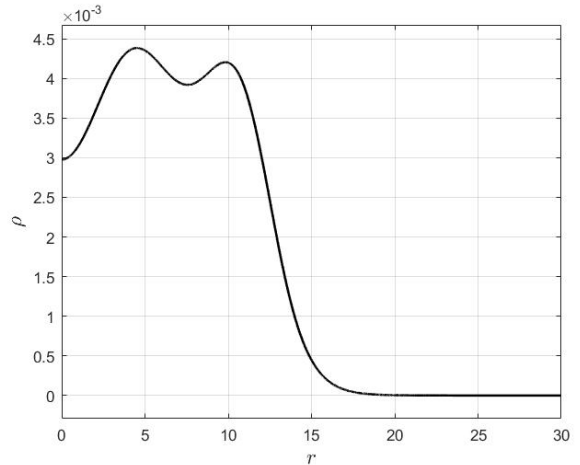


$$E = -23.878\,929\,940\,18$$

(b) Non-interacting solution on the left and Kohn-Sham solution on the right for $N = 20$.



$$E = -159.312\,790\,499\,91$$



$$E = -74.220\,175\,617\,02$$

(c) Non-interacting solution on the left and Kohn-Sham solution on the right for $N = 40$.

Figure 5: Energy and density for different sodium clusters.

One may notice that in general the Kohn-Sham solution leads to a smaller density close the origin due to the effect of the repulsion of the electrons, neglected in the non-interacting model.

This repulsion also leads to a positive contribution to the total energy of the cluster; in general the Kohn-Sham energies are about one half of the ones obtained in the non-interacting approximation.

Polarizability of metal clusters

It is possible to estimate the polarizability of a metal cluster from the electron spillout, which is defined as

$$\delta N = \int_{R_c}^{\infty} \rho(r) 4\pi r^2 dr \quad (31)$$

The polarizability estimation is then given by

$$\alpha(N) = R_c^3 \left(1 + \frac{\delta N}{N} \right) \quad (32)$$

We use the density ρ found with the method illustrated in the previous section. We do it for different elements:

	Li	Na	K	Rb	Cs
R_s [a_0]	3.26	3.93	4.86	5.20	5.62

Table 3: Wigner-Seitz radii of some alkali metals.

In the following Table 4, we show the clusters polarizability $\alpha(N)$ for the various clusters we have worked out.

	$N = 8$	$N = 20$	$N = 40$
α_{Li}	337.959	811.486	1584.31
α_{Na}	578.177	1395.82	2732.80
α_{K}	1066.25	2588.36	5082.65
α_{Rb}	1295.99	3151.14	6193.20
α_{Cs}	1622.08	3951.05	7771.57

Table 4: Clusters polarizability for different clusters of alkali metals.

We can compare our results for $N = 20$ with the polarizability computed from the δN data reported in a paper by N. Van Giai³

	$N = 20$
α_{Li}	807.3
α_{Na}	1390
α_{K}	2583
α_{Rb}	3136
α_{Cs}	3941

Table 5: Clusters polarizability for $N = 20$ from N. Van Giai paper.

Ours and N. Van Giai results differ by less than 0.6%, which is an excellent agreement considering that they presented the δN data with only two significant digits. Nevertheless, a difference

³N. Van Giai, Progress of Theoretical Physics Supplement No. 124, (1996)

in the calculations must be remarked: a different parametrization of ϵ_c has been used in the paper, namely they used Wigner's version

$$\epsilon_c = -\frac{0.88}{7.8 + r_s} \quad \Rightarrow \quad \frac{\delta E_c}{\delta \rho} = \frac{\epsilon_c}{3} \left(\frac{23.4 + 4r_s}{7.8 + r_s} \right) \quad (33)$$

while in our analysis we used the Perdew-Zunger parametrization

$$\epsilon_c = \frac{\gamma}{1 + \beta_1 \sqrt{r_s} + \beta_2 r_s} \quad \Rightarrow \quad \frac{\delta E_c}{\delta \rho} = \frac{\epsilon_c}{6} \left(\frac{6 + 7\beta_1 \sqrt{r_s} + 8\beta_2 r_s}{1 + \beta_1 \sqrt{r_s} + \beta_2 r_s} \right) \quad (34)$$

To better understand the difference in dynamics of electrons given by the different parametrization of correlation energy, in Figure 6 we compare the value of correlation potentials.

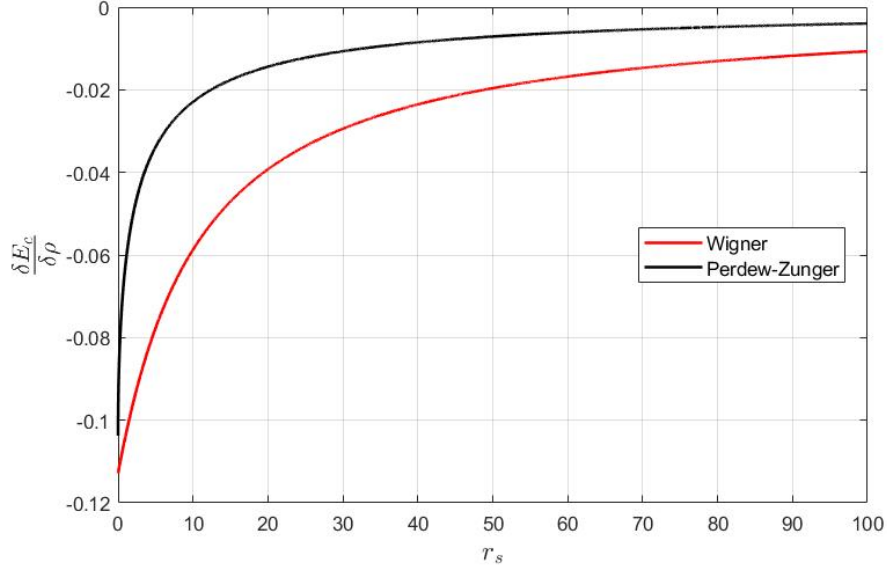


Figure 6: Comparison between Perdew-Zunger and Wigner correlation potentials

Wigner's correlation potential has always lower values than Perdew-Zunger's, which means that electrons modelled in Van Giai's paper feel a stronger attraction than those we modelled. Therefore we can figure electron clouds in Van Giai's clusters are denser at the center of the modelled cluster while, using Perdew-Zunger parametrization, electrons distribute in a wider way around ions. Henceforth the amount of electrons beyond cluster's size R_c is greater, that is δN is bigger leading to a larger polarizability in our case.